DOI: 10.15669/pnst.7.74

Progress in Nuclear Science and Technology
Volume 7 (2025) pp. 74-77

ARTICLE

A new detection method of charged-particle emission reactions for the development of molten salt reactors

Tatsuya Katabuchi *, Takaaki Ogiso, Hideto Nakano and Yu Kodama

Laboratory for Zero-Carbon Energy, Institute of Innovative Research, Tokyo Institute of Technology, 2-12-1 Ookayama, Meguro-ku, Tokyo 152-8550, Japan

A new detection method for measurement of neutron-induced charged-particle emission reactions was developed. In the new method, a sample-added plastic scintillator is used. The process to fabricate plastic scintillator added with sample material was established. The scintillators were tested with a neutron beam at the Japan Proton Accelerator Research Complex. Particle identification was attempted by the pulse-shaping discrimination technique and charged-particle emission events were successfully detected with a good separation from γ-ray background.

Keywords: ***nuclear data; neutron; charged-particle emission reaction; molten salt reactor; radiation measurement***

1. Introduction

Molten salt reactors have attracted great attention because of several beneficial characteristics in recent years. Projects to study molten salt reactors started and are ongoing in many countries. Research reveals that neutron-induced charged-particle emission reactions such as (n,p), (n,α), occurring in elements included in molten salt (F, Li, Be, K, Cl etc.), are important for the design of reactor cores [1-4]. However, neutron-induced charged-particle emission reactions have not been measured as extensively and systematically as the total and neutron capture reactions. Current charged-particle emission reaction cross section data of some elements, for example, chlorine, do not satisfy demand for reactor core design of molten salt reactors [5]. Most of the past measurements have been made in the MeV neutron energy region. The cross-section data in the wide energy range from thermal to keV are required for applications. In addition, the traditional experimental method, in which a thin layer sample is irradiated with neutrons and charged particles from the thin sample are detected with semiconductor detectors as shown in **Figure 1**, limits the thickness of samples due to the energy loss of charged-particles in the samples, resulting in low counting statistics.

To solve this issue and achieve higher statistics than the traditional method, we are developing a new method to measure cross sections of neutron-induced charged-particle reactions. The new method adopts a sample-loaded scintillator instead of a thin layer sample as depicted in **Figure 2**. Sample material for measurement is loaded into organic scintillator material and thin scintillators are fabricated. In this method, sample and detector are combined. The sample-loaded scintillator is irradiated with neutron beam and charged particles from nuclear reactions deposit their energies in the scintillator, inducing scintillation photons that are detected with a photomultiplier tube. This method allows us to increase the amount of sample, leading to higher statistics of detected counts. Additionally, plastic scintillators enable the utilization of the pulse-shape discrimination technique for distinguishing between different types of particles. This technique is rooted in the principle that scintillation light emission from organic materials like plastic and liquid scintillators exhibit distinct decay constants corresponding to various particle types. Specifically, the decay time constant becomes slower as the mass of the particle increases. Consequently, it becomes possible to differentiate the detected particle types by analyzing the profile of the light emission signal produced

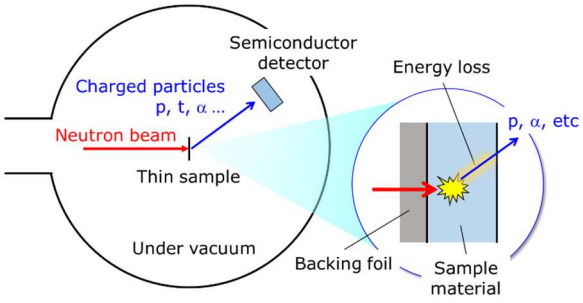

Figure 1. Traditional method to measure neutron-induced charged-particle emission reactions.

*Corresponding author. E-mail: buchi@zc.iir.titech.ac.jp

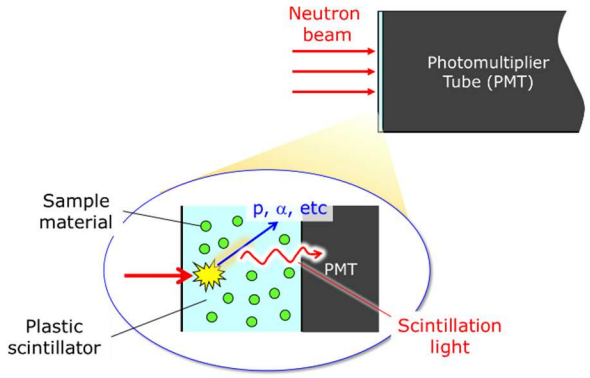

Figure 2. Schematic concept of new detection system for measurement of neutron-induced charged-particle emission reactions.

by the scintillator. We fabricated the scintillator and tested it with neutron beams at the Pelletron accelerator of Tokyo Tech and the Japan Proton Accelerator Research Complex (J-PARC).

2. Fabrication

A process to fabricate plastic scintillator including a sample material for measurement was developed. Photocurable-resin was used as a base material of the scintillator. After mixing the scintillator and the sample material, the mixture is cured by irradiation with ultraviolet light. This allows us to add even an insoluble substance to scintillator, which precipitates in liquid scintillator and thereby does not distribute uniformly. The uniform distribution of the added substance in photocurable-resin-based scintillator can be achieved by UV curing that immobilizes the substance after stirring the mixture of the scintillator and the substance.

Figure 3 shows the structure of the fabricated plastic scintillator schematically. The fabricated scintillator is disk-shaped and formed in a circular plastic frame. The front and the back sides are covered with 12-μm Mylar films. The diameter of the scintillator is 20 mm or 10 mm. The thickness is 1 mm.

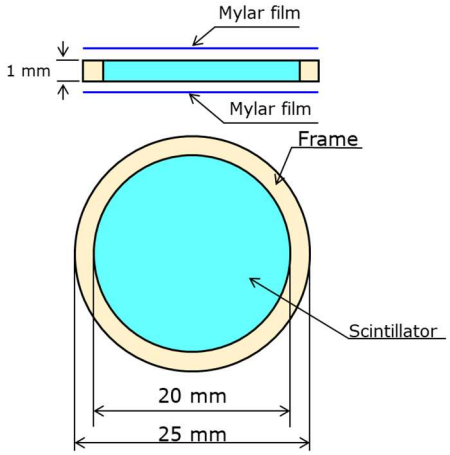

Figure 3. Structure of scintillator.

The fabrication process is shown in **Figure 4**. The scintillator was fabricated as follows. (1) The bottom Mylar film was glued to the frame. (2) Scintillator resin added with the sample material was filled into the frame. (3) The upper side of the scintillator was covered with a Mylar film to seal the scintillator. (4) The scintillator resin was cured by irradiation with UV light.

Substances listed in **Table 1**, LiF, $B(OH_3)$ and KI, were chosen to add to the scintillator for test experiments. Lithium-6 in the LiF sample was isotopically enriched. Lithium-6 and boron-10 have large reaction cross sections with neutrons. The $^{6}Li(n,t)^{4}He$ reaction emits a triton and an alpha particle. The $^{10}B(n,\alpha)^{7}Li$ reaction emits an alpha particle and a ^{7}Li nucleus. These high-energy charged-particles are good for experiments to test the fabricated scintillator. The attained areal densities of the added samples were roughly ten times greater than those of the thin foil samples employed in the conventional measurements.

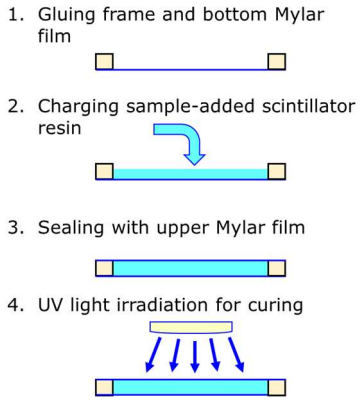

Figure 4. Fabrication process of sample-added scintillator.

Table 1. Fabricated sample-added scintillator.

Added sample material	Possible reactions (Q-values)
Pure scintillator	
^{6}LiF	$^{6}Li(n,t)^{4}He$ (4.78 MeV)
$B(OH_3)$	$^{10}B(n,\alpha)^{7}Li$ (2.79 MeV)
KI	$^{127}I(n,\alpha)^{124}Sb$ (4.28 MeV), $^{39}K(n,\alpha)^{36}Cl$ (1.36 MeV)

3. Experiments

Experiments were performed using a pulsed-neutron beam from a spallation neutron source of the Materials and Life Science Facility (MLF) in J-PARC. The sample-added scintillators were irradiated with neutrons at a neutron beam line, the Accurate Neutron-Nucleus Reaction Instrument (ANNRI) of MLF/J-PARC [7]. **Figure 5** shows the layout of ANNRI. The scintillation detector was

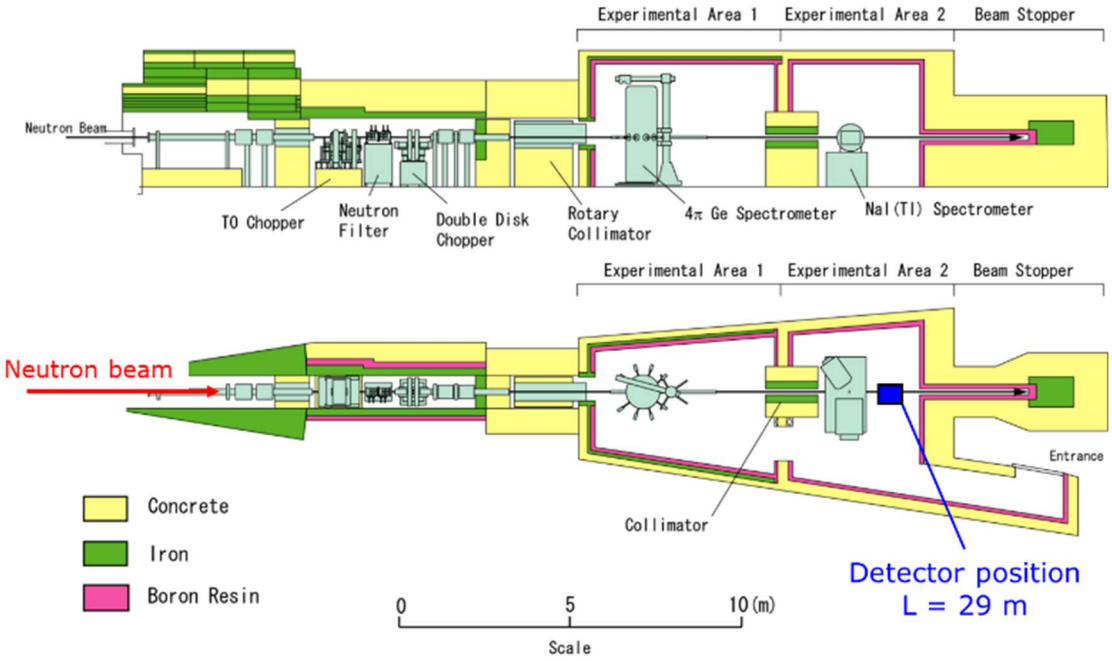

Figure 5. Accurate Neutron-Nucleus Reaction Measurement Instrument.

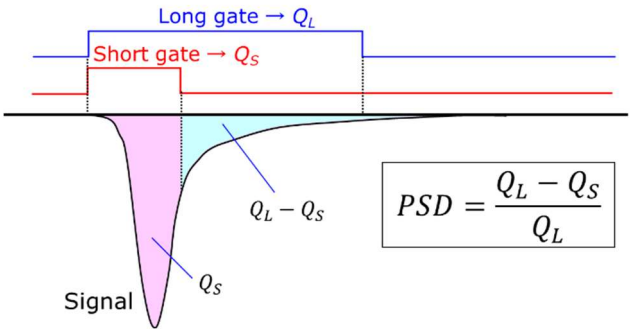

Figure 6. Gate setting for pulse shape discrimination.

placed at a flight distance of 29 m from the neutron source. The neutron energy of the incident neutron was measured by the time-of-flight (TOF) method.

The anode signal from the photomultiplier tube of the scintillation detector was fed into a data acquisition system (CAEN V1720). The data acquisition system registered the TOF and integrated areas of the signal over two different time intervals denoted as "long" and "short" gates in **Figure 6**. As mentioned earlier, the time evolution of light emission from organic scintillator depends on the particle mass. The light output of heavier particles has longer decay time. In the data analysis, the decay time of the detected signal was evaluated by calculating the quantity $PSD = (Q_L - Q_S)/Q_L$, where Q_L and Q_S are integrated areas of the signal for the long and short gates, respectively.

4. Results and discussion

Two-dimensional plots of the pulse height vs PSD of the experimental results are shown in **Figure 7**. The plots for the ^{6}LiF-added and B(OH)$_3$-added scintillators have high counts in different regions from the pure scintillator. Major events for the pure scintillator are γ-rays. The PSD of the γ-ray events is a little lower than 0.2. On the other hand, the high-count region for the ^{6}LiF-added scintillator appears above 0.2 in PSD. These events are attributed to tritons from the ^{6}Li(n,t)^{4}He reaction. The plot for the B(OH)3-added scintillator also shows a distinct high-count region in a different place from γ-rays but the pulse-height is very small. The events must be alpha particles from the ^{10}B(n,α)^{7}Li reaction. The small pulse-height of the output is caused by the property of organic scintillator that the light emission efficiency decreases with the mass of particles. Further investigations are required to differentiate between charged particle and γ-ray emission events in the KI data.

5. Conclusion

For measurement of neutron-induced charged-particle emission reactions, a new detection method, in which a sample-added plastic scintillator is used, was developed. The process to fabricate plastic scintillator including sample material was established. The fabricated scintillators were tested with a neutron beam at the Japan Proton Accelerator Research Complex. Particle identification was attempted by the pulse-shaping discrimination technique. Charged-particle emission events were successfully detected with a good separation from γ-ray background. It is concluded that the present detector can be used for measurement of

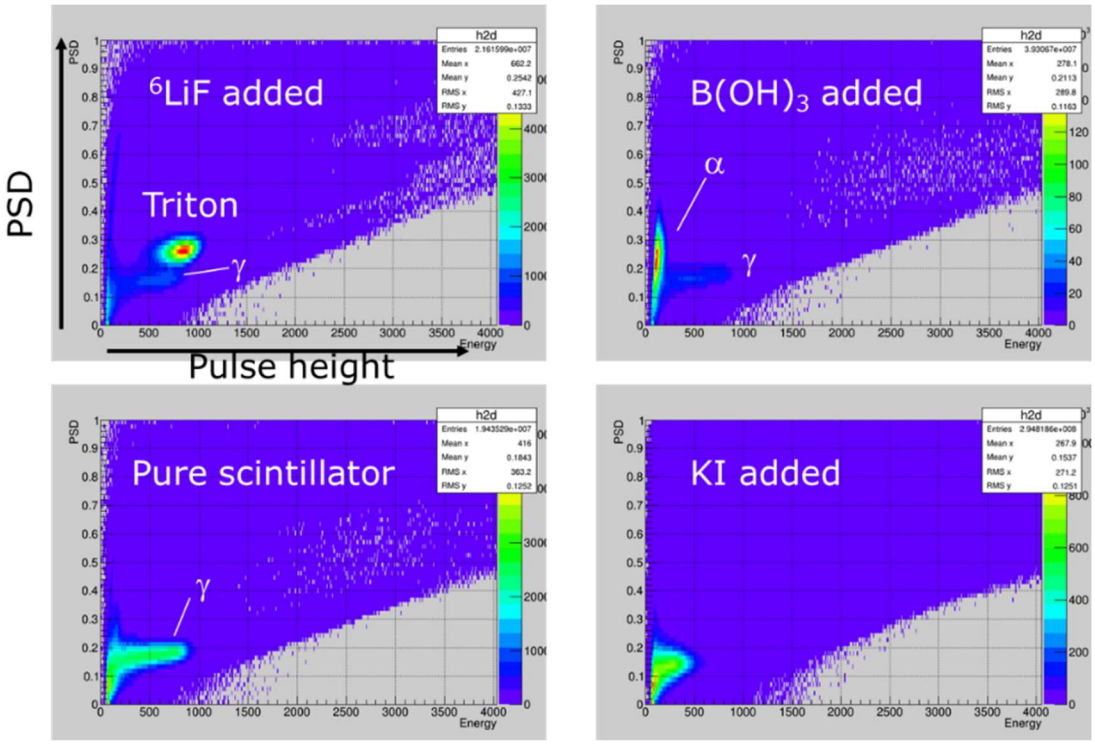

Figure 7. Two-dimensional plots of pulse height vs ***PSD*** for sample-added scintillator.

neutron-induced charged-particle emission reactions in the future experiments.

Acknowledgements

This work was supported by the MEXT Innovative Nuclear Research and Development Program.

References

[1] E. Sansarbayar, et al., Cross sections for the ^{35}Cl(n,α)^{32}P reaction in the 3.3–5.3 MeV neutron energy region, Physical Review C 104 (2021), 044620.

[2] S.A. Kuvin, et al., Nonstatistical fluctuations in the ^{35}Cl(n,p)^{35}S reaction cross section at fast-neutron energies from 0.6 to 6 MeV, *Physical Review C* 102 (2020), 024623.

[3] J.C. Batchelder et al., Possible evidence of nonstatistical properties in the ^{35}Cl(n, p)^{35}S cross section, *Physical Review C* 99 (2019), 044612.

[4] P.E. Koehler, ^{35}Cl(n,p)^{35}S cross section from 25 meV to 100 keV, *Physical Review C* 44 (1991), 1675.

[5] M. Kawaguchi, et al., Uncertainty analysis of transmutation properties of Chloride molten salt fast reactors due to uncertainties in nuclear data of ^{35}Cl by a random sampling method, *Annual Meeting of the Atomic Energy Society of Japan*, March 2022.

[6] K. Kino, et al., Measurement of energy spectra and spatial distributions of neutron beams provided by the ANNRI beamline for capture cross section measurements at the J-PARC/MLF, *Nuclear Instruments and Methods*, A 626 (2011), p. 58.